CrystEngComm

Accepted Manuscript

ROYAL SOCIETY OF CHEMISTRY

www.rsc.org/crystengcomm

Controllable Synthesis of Four Series of Lanthanide Coordination Polymers: Synthesis, Structures, Luminescent and Magnetic Properties

Ran An, Xiaofang Wang, Huai-Ming Hu*, Zhui Zhao, Chao Bai, Ganglin Xue

Key Laboratory of Synthetic and Natural Functional Molecule Chemistry of Ministry of Education, College of Chemistry and Materials Science, Northwest University, Xi'an 710127, China

ABSTRCT: Four series of new lanthanide coordination polymers, namely, $[LnL(glu)]_n \cdot 2nH_2O$ (Ln=Nd (**1**), Sm (**2**), Gd (**3**)), $[YbL(glu)]_n$ (**4**), $[LnL(glu)(H_2O)]_n$ (Ln=Pr (**5**), Sm (**6**), Gd (**7**), Dy (**8**), Ho (**9**), Er (**10**), Y(**11**)), $[PrL(glu)(H_2O)]_n$ (**12**) [HL = (2-(2-sulfophenyl)imidazo(4,5-f)(1,10)-phenanthroline, H_2glu = glutaric acid] have been hydrothermally synthesized and characterized by elemental analysis, IR spectra and single crystal X-ray diffraction. Isostructural compounds **1-3** exhibit 6-connected 3D network with the topological type of ***pcu***, containing left- and right-handed helical chains. Compound **4** is a 6-connected 3D network with ***bsn*** topology, which contains unique meso-helical chains. Because of the lanthanide contraction, compounds **1-3** and **4** show different structures, which are all synthesized at the pH=4.0 and the molar ratio of Ln^{III}:HL:H_2glu=2:1:1. When only change the pH value to 6.0, isostructural compounds **5-11** show 4-connected 2D ***sql*** topology with the point symbol of $(4^4 \cdot 6^2)$. By changing the molar ratio of 2:1:1 (Ln^{III}: HL: H_2glu) to 2:1:2 at pH= 4.0, compound **12** shows an 8-connected 3D network with ***bcu*** topology which has left- and right-handed helical chains. Photoluminescence spectra of compounds **1-12** have been investigated upon excitation at 370 nm. Magnetic susceptibility measurements exhibit typical paramagnetic behavior for compounds **3** and **7**, weak antiferromagnetic interactions for compounds **8-10**.

INTRODUCTION

Research on lanthanide coordination polymers has become a hot field and made considerable headway due to their fascinating topologies, multifunctional magnetic materials and luminescence for functional materials and bio-sciences.[1] Nevertheless, it is still a challenge to design and synthesize lanthanide coordination polymers with high dimensions and excellent properties, because of Ln^{III} cations with high and variable coordination numbers and diverse coordination geometries, which can lead to fantastic structures. Thus the rational choice of organic ligands is particularly important in construction of expected lanthanide coordination polymers.[2] Moreover, the pH and molar ratio of the reactants may affect the type of meso-phases, leading to different structures.[3] Recently, many 1,10-phenanthroline derivatives have been used to construct lanthanide coordination polymers as a rational choice with good luminescence properties (such as white light emitting materials introducing single dopant and codopants),[4] novel functionalized mesoporous nanosphere materials[5] as well as single-molecular magnets[1a,6], in which 1,10-phenanthroline derivatives can transfer and sensitize Ln^{III} ions effectively. However, synthesis conditions of lanthanide coordination polymers based on 1,10-phenanthroline derivatives are still scarce and shall not cease from exploration. Therefore we pay more attention to better control of synthesis conditions and the influence of lanthanide contraction on the diversity of lanthanide coordination polymers.

Recently, our group has reported coordination polymers with 2-(2,4-disulfophenyl)imidazo(4,5-f)(1,10)-phenanthroline and 2-(2-carboxyphenyl) imidazo(4,5-f)(1,10)-phenanthroline.[3b,7] In this paper, we report four series of lanthanide coordination polymers based on 2-(2-sulfophenyl)imidazo(4,5-f) (1,10)-phenanthroline (HL) and glutaric acid (H_2glu) ligands. The considerations that we have are as follows: (1) the glutaric acid is a flexible ligand and very beneficial to the formation and extension of high dimension structures by bridging Ln^{III} ions.[8] (2) the multidentate HL ligand has the bidentate phenanthroline and the terminal sulfonic group, which shows various coordination modes.[4,9] The conjugated system is not only an excellent chromophore, an effective absorbing sensitizer, but also can improve the rigidity of compounds.[10] Based on the above, we hydrothermally synthesized four series of lanthanide coordination polymers by controlling the pH value and

metal-to-ligand ratios at the same temperature. The four series compounds, namely, $[LnL(glu)]_n \cdot 2nH_2O$ (Ln=Nd (**1**), Sm (**2**), Gd (**3**)), $[YbL(glu)]_n$ (**4**), $[LnL(glu)(H_2O)]_n$ (Ln=Pr (**5**), Sm (**6**), Gd (**7**), Dy (**8**), Ho (**9**), Er (**10**), Y(**11**)), $[PrL(glu)(H_2O)]_n$ (**12**) show obvious influence of the lanthanide contraction on the coordination number and crystal structures, and in which HL ligand show two coordination modes as shown in Scheme 1. Herein, we reveal the synthesis, structures, visible and near-infrared luminescence as well as the magnetic properties of these lanthanide coordination polymers in details.

Scheme 1 is here

EXPERIMENTAL SECTION

Materials and Methods. The ligand HL was prepared from 1,10-phenanthroline according to literature methods.[7] Hydrated $Ln(NO_3)_3$ salt were synthesized by dissolving Ln_2O_3 or Tb_4O_7(99.99%) in concentrated nitric acid. All other chemicals were reagent grade and used as received without any further purification. IR spectra were recorded on a Bruker EQUINOX-55 Fourier transform Infrared spectrometer in the range of 4000 to 400 cm^{-1} using KBr pellets. Elemental analyses (C, H, N) were performed using an elementar Vario EL elemental analyzer. TGA were conducted on a Universal V2.6 DTA system by heating up from 30 to 900 °C at 10 °C/min. PXRD measurements were performed on a Bruker D8 ADVANCE X-ray powder diffractometer with Cu-Kα (1.5418 Å). Fluorescence spectra for the solid samples were recorded at room temperature on a Hitachi F-4500 spectrophotometer. The near-infrared spectra were performed on an Edinburgh FLS920 fluorescence spectrometer in the range of 800−1700 nm. The variable-temperature magnetic susceptibilities in the temperature range of 1.8-300 K were measured on a Quantum Design MPMS-7 SQUID magnetometer in a field of 1000 Oe. Diamagnetic corrections were made with Pascal's constants for all of the constituent atoms.

Synthesis of $[NdL(glu)]_n \cdot 2nH_2O$ (1) $Nd(NO_3)_3 \cdot 6H_2O$ (87.67 mg, 0.2 mmol), HL(37.64 mg, 0.1 mmol), H_2glu (13.21 mg, 0.1 mmol) and H_2O (10 mL) were mixed and stirred for 30 min at room temperature. And then the acidity of the mixture was adjusted to pH 4.0 with 0.5 mol L^{-1} NaOH solution. The reactants above were sealed

in a 25 mL Teflon-lined stainless steel autoclave and maintained at 180 °C for 3 days. When cooling to room temperature, pale yellow block crystals were obtained. Yield: 29.2 mg (42.6%) based on HL. Anal. Calcd.(%) for $C_{24}H_{21}NdN_4O_9S$ (685.75): C, 42.03; H, 3.09; N, 8.17%. Found: C, 41.71; H, 2.83; N, 8.22%. IR (KBr, cm^{-1}): 3430(w), 3216(vw), 3084(vw), 1585(vs), 1550 (vw),1421(s), 1348(vw), 1272(vw), 1219(w), 1184(m), 1132(w), 1084(m), 1013(m), 880(vw), 815(m), 793(w), 745(s), 700(m), 615(s), 558(m)

Synthesis of $[SmL(glu)]_n \cdot 2nH_2O$ (2) Compound **2** was synthesized by a method similar to that of **1**, except that $Nd(NO_3)_3 \cdot 6H_2O$ was replaced by $Sm(NO_3)_3 \cdot 6H_2O$ accordingly. Light yellow crystals of **2** were obtained, yield: 37.5 mg (54.2%) based on HL. Anal. Calcd.(%) for $C_{24}H_{21}SmN_4O_9S$ (691.87): C, 41.66; H, 3.06; N, 8.10%. Found: C, 41.21; H, 2.83; N, 8.22%. IR (KBr, cm^{-1}): 3432(w), 3218(vw), 3086(vw), 1588(vs), 1548(vw),1424(s), 1350(vw), 1275(vw), 1222(w), 1180(m), 1134(w), 1084(m), 1015(m), 883(vw), 816(m), 790(w), 740(s), 701(m), 618(s), 560(m)

Synthesis of $[GdL(glu)]_n \cdot 2nH_2O$ (3) The synthetic process of **1** and **3** is similar, just change $Nd(NO_3)_3 \cdot 6H_2O$ to $Gd(NO_3)_3 \cdot 6H_2O$. Yellow crystals of **3** were obtained, yield: 28.5 mg (40.8%) based on HL. Anal. Calcd.(%) for $C_{24}H_{21}GdN_4O_9S$ (698.76): C, 41.25; H, 3.03; N, 8.02%. Found: C, 41.19; H, 2.81; N, 8.19%. IR (KBr, cm^{-1}): 3429(w), 3215(vw), 3084(vw), 1590(vs), 1550(vw),1425(s), 1346(vw), 1273(vw), 1219(w), 1184(m), 1133(w), 1086(m), 1017(m), 8835(vw), 817(m), 793(w), 736(s), 7021(m), 617(s), 558(m)

Synthesis of $[YbL(glu)]_n$ (4) The synthetic process of **4** is similar to **1**, except that $Nd(NO_3)_3 \cdot 6H_2O$ was replaced by $Yb(NO_3)_3 \cdot 6H_2O$ accordingly. Pale yellow block crystals were obtained, yield: 39.8 mg (58.6%) based on HL. Anal. Calcd.(%) for $C_{24}H_{17}YbN_4O_7S$ (678.52): C, 42.48; H, 2.53; N, 8.26%. Found: C, 42.61; H, 2.65; N, 8.15%. IR (KBr, cm^{-1}): 3422(m), 3091(w), 2973(w), 2944(w), 1632(vs), 1582(vw), 1547(w), 1455(w), 1418(m), 1361(w), 1262(s), 1188(w), 1154(s), 1130(w), 1083(m), 1018(s), 950(w), 807(m), 783(w), 745(s), 703(m), 614(s), 557(m)

Synthesis of $[PrL(glu)(H_2O)]_n$ (5) $Pr(NO_3)_3 \cdot 6H_2O$ (87.00 mg, 0.2 mmol), HL(37.64 mg, 0.1 mmol), H_2glu (13.21 mg, 0.1 mmol) and H_2O (10 mL) were mixed and stirred for 30 min at room temperature. And then the acidity of the mixture was adjusted to pH 6.0 with 0.5 mol L^{-1} NaOH solution. The reactants above was sealed in

a 25 mL Teflon-lined stainless steel autoclave and maintained at 180 °C for 3 days. When cooling to room temperature, pale yellow columnar crystals were obtained, yield: 38.7 mg (58.3%) based on HL. Anal. Calcd.(%) for $C_{24}H_{19}PrN_4O_8S$ (664.40): C, 43.38; H, 2.88; N, 8.43%. Found: C, 43.21; H, 2.73; N, 8.14%. IR (KBr, cm^{-1}): 3384(w), 3268(vw), 3072(w), 2975(w), 1668(w), 1583(vs), 1542(w), 1455(w), 1420(s), 1242(s), 1171(vs), 1135(m),1085(s), 1057(m), 1025(s), 944(m), 812(s), 736(s), 705(m), 654(m), 556(m), 490(m)

Synthesis of $[SmL(glu)(H_2O)]_n$ (6) The synthetic process of **6** is similar to **5**, except that $Pr(NO_3)_3·6H_2O$ was replaced by $Sm(NO_3)_3·6H_2O$ accordingly. When cooling to room temperature, yellow block crystals were obtained, yield: 37.8 mg (56.1%) based on HL. Anal. Calcd.(%) for $C_{24}H_{19}SmN_4O_8S$ (673.85): C, 42.78; H, 2.84; N, 8.31%. Found: C, 42.51; H, 2.93; N, 8.14%. IR (KBr, cm^{-1}): 3387(w), 3267(vw), 3072(w), 2973(w), 1690(w), 1582(vs), 1540(w), 1456(w), 1419(s), 1241(s), 1170(vs), 1137(m), 1086(s), 1055(m), 1024(s), 943(m), 814(s), 735(s), 704(m), 655(m), 558(m), 487(m)

Synthesis of $[GdL(glu)(H_2O)]_n$ (7) The synthetic process of **7** is similar as **5**, except that $Pr(NO_3)_3·6H_2O$ was replaced by $Gd(NO_3)_3·6H_2O$ accordingly. When cooling to room temperature, yellow block crystals were obtained, yield: 39.3 mg (57.7%) based on HL. Anal. Calcd.(%) for $C_{24}H_{19}GdN_4O_8S$ (680.74): C, 42.34; H, 2.81; N, 8.23%. Found: C, 42.28; H, 2.91; N, 8.16%. IR (KBr, cm^{-1}): 3385(w), 3266(vw), 3070(w), 2971(w), 1688(w), 1581(vs), 1539(w), 1455(w), 1418(s), 1240(s), 1171 (vs), 1136(m), 1089(s), 1056(m), 1023(s), 940(m), 815(s), 733(s), 704(m), 653(m), 559(m), 488(m)

Synthesis of $[DyL(glu)(H_2O)]_n$ (8) The synthetic process of **8** is similar as **5**, except that $Pr(NO_3)_3·6H_2O$ was replaced by $Dy(NO_3)_3·6H_2O$ accordingly. When cooling to room temperature, yellow crystals were obtained, yield: 39.6 mg (57.7%) based on HL. Anal. Calcd.(%) for $C_{24}H_{19}DyN_4O_8S$ (685.99): C, 42.02; H, 2.79; N, 8.17%. Found: C, 42.08; H, 2.91; N, 8.11%. IR (KBr, cm^{-1}): 3388(w), 3072(w), 2976(w), 2190(vw), 1668(w), 1584(vs), 1543(w), 1456(w), 1421(s), 1244(s), 1172(vs), 1133(m), 1087(s), 1054(m), 1026(s), 946(m), 810(s), 735(s), 704(m), 657(m), 556(m), 483(m)

Synthesis of $[HoL(glu)(H_2O)]_n$ (9) The synthetic process of **9** is similar as **5**, except that $Pr(NO_3)_3·6H_2O$ was replaced by $Ho(NO_3)_3·6H_2O$ accordingly. When cooling to room temperature, small yellow crystals were obtained, yield: 35.2 mg (51.2%) based on HL. Anal. Calcd.(%) for $C_{24}H_{19}HoN_4O_8S$ (688.43): C, 41.87; H, 2.78; N, 8.14%. Found: C, 41.69; H, 2.87; N, 8.09%. IR (KBr, cm^{-1}): 3380(w), 3264(vw), 3068(w), 2970(w), 1685(w), 1583(vs), 1536(w), 1453(w), 1414(s), 1239(s), 1168(vs), 1134(m), 1090(s), 1054(m), 1022(s), 943(m), 815(s), 732(s), 703(m), 652(m), 561(m), 490(m)

Synthesis of $[ErL(glu)(H_2O)]_n$ (10) The synthetic process of **10** is similar as **5**, except that $Pr(NO_3)_3·6H_2O$ was replaced by $Er(NO_3)_3·6H_2O$ accordingly. When cooling to room temperature, yellow diamond crystals were obtained, yield: 33.0 mg (47.8%) based on HL. Anal. Calcd.(%) for $C_{24}H_{19}ErN_4O_8S$ (690.75): C, 41.73; H, 2.77; N, 8.11%. Found: C, 41.62; H, 2.83; N, 8.06%. IR (KBr, cm^{-1}): 3378(w), 3262(vw), 3069(w), 2968(w), 1688(w), 1584(vs), 1537(w), 1454(w), 1415(s), 1238(s), 1171(vs), 1136(m), 1089(s), 1056(m), 1024(s), 945(m), 816(s), 735(s), 702(m), 653(m), 563(m), 491(m)

Synthesis of $[YL(glu)(H_2O)]_n$ (11) The synthetic process of **11** is similar as **5**, except that $Pr(NO_3)_3·6H_2O$ was replaced by $Y(NO_3)_3·6H_2O$ accordingly. When cooling to room temperature, yellow diamond crystals were obtained, yield: 28.35 mg (46.3%) based on HL. Anal. Calcd.(%) for $C_{24}H_{19}YN_4O_8S$ (612.40): C, 47.07; H, 3.13; N, 9.15%. Found: C, 41.62; H, 2.83; N, 8.06%. IR (KBr, cm^{-1}): 3381(w), 3266(vw), 3070(w), 2967(w), 1689(w), 1583(vs), 1536(w), 1457(w), 1417(s), 1236(s), 1172(vs), 1137(m), 1088(s), 1057(m), 1026(s), 948(m), 817(s), 737(s), 701(m), 654(m), 564(m), 487(m)

Synthesis of $[PrL(glu)(H_2O)]_n$ (12). $Pr(NO_3)_3·6H_2O$ (87.00 mg, 0.2 mmol), HL(37.64 mg, 0.1 mmol), H_2glu (26.42 mg, 0.2 mmol) and H_2O (10 mL) were mixed and stirred for 30 min at room temperature. And then the acidity of the mixture was adjusted to pH 4.0 with 0.5 mol L^{-1} NaOH solution. The reactants above was sealed in a 25 mL Teflon-lined stainless steel autoclave and maintained at 180 °C for 3 days. When cooling to room temperature, pale yellow block crystals of compound **12** were obtained, yield: 39.7mg (59.8%). based on HL. Anal. Calcd.(%) for $C_{24}H_{19}PrN_4O_8S$ (664.40): C, 43.38; H, 2.88; N, 8.43%. Found: C, 43.42; H, 2.61; N, 8.31%. IR (KBr,

cm^{-1}): 3743 (vw), 3198(s), 3057(w), 2958(w), 2887(w), 1591(vs), 1544(w), 1511(vw), 1456(m), 1435(w), 1411(vs), 1357(w), 1186(vs), 1139(m), 1080(s), 1016(vs), 884(w), 817(s), 737(s), 663(m), 638(w), 561(m)

Scheme 2 is here

X-ray crystallography. Diffraction data for compounds **1-12** were collected using a Bruker Smart APEX II CCD diffractometer with graphite-monochromated Mo-K_α radiation (λ = 0.71073 Å) at room temperature. Empirical absorption corrections were applied based on the SADABS program. The structures were solved by direct methods and the heavy atom method and refined by the full-matrix least-squares based on F^2 using SHELXTL-97. All non-hydrogen atoms were refined anisotropically. Hydrogen atoms of organic ligands were generated geometrically. Selected crystal data and structural refinement parameters for compounds **2**, **4**, **6**, **12** are listed in Table 1 and the others are summarized in Table S1 (Supporting Information). Selected bond distances and bond angles are summarized in Table S2. Crystallographic data have been deposited with the Cambridge Crystallographic Data Centre, CCDC Nos: 1414374-1414385. These data can be obtained free of charge via www.ccdc.can.ac.uk/conts/retrieving.html (or from the Cambridge Crystallographic Centre, 12 Union Road, Cambridge CB2 1EZ, U.K., fax (+44) 1223–336033, or deposit @ccdc.cam.ac.uk).

Table 1 is here

RESULTS AND DISCUSSION

Description of crystal structures

Crystal Structure of $[LnL(glu)]_n \cdot 2nH_2O$ (Ln=Nd (**1**), Sm (**2**), Gd (**3**)). X-ray crystallography reveals that compounds **1**, **2** and **3** are an isomorphic 3D framework and crystallized in the monoclinic $P2_1/n$ space group. Take compound **2** as an example, its asymmetric unit contains one independent Sm^{III} cation, one L^- ligand, one glu^{2-} anion and two lattice water molecules. The nona-coordinated Sm^{III} cation is a

distorted tricapped trigonal prism coordination geometry formed by two nitrogen atoms (N1, N2) and two oxygen atoms (O1B, O2B) from L^- ligand, five O atoms (O4, O4A, O5, O6C, O7D) from glu^{2-} ligands (Figure 1a). The Sm-N and Sm-O bond lengths vary from 2.570(3) to 2.641(3) Å and 2.316(2) to 2.745(3) Å, respectively, and the angles of O-Sm-O and O-Sm-N range from 50.91(8)-139.01(8)º and 50.91(8)-156.60(8)º, which are similar to those reported in other Sm^{III} compounds.[11] Adjacent Sm^{III} cations form a noteworthy paddle-wheel $[Sm_2O_2(CO_2)_2]$ subunit with Sm···Sm distance of 3.9606(5) Å bridged by carboxylate group. $[Sm_2O_2(CO_2)_2]$ subunits are bridged by L^- ligands exhibiting the μ_2-η^2:η^2 mode (Scheme 1a) to form left- and right-handed helical chains of $[SmL^-]_\infty$ with a pitch of 14.916 Å, giving rise to an achiral 2D layer along the a-axis (Figure 1b). Finally, each binuclear $[Sm_2O_2(CO_2)_2]$ subunit of the 2D layer is connected by two glu^{2-} ligands to produce a 3D framework along the b-axis (Figure 1c). Besides, intermolecular hydrogen bonding interactions between lattice water molecules and L^- ligands make the 3D framework much stable (N3-H3A···O3=2.734 Å, 143.11°). In order to make clear the analysis of the structure, we can define the $[Sm_2O_2(CO_2)_2]$ subunits as 6-connected nodes as shown in Figure 2d. The simplified structure is a 6-connected ***pcu*** topology with the point symbol of $(4^{12}\cdot6^3)$ (Figure 2e).

Figure 1 is here

Crystal Structure of $[YbL(glu)]_n$ (**4**). X-ray analysis reveals compound **4** is a 3D network and crystallized in the orthorhombic system with Fdd2 space group. The asymmestric unit contains one independent Yb^{III} cation, one L^- ligand and one glu^{2-} anion. As illustrated in Figure 2a, the seven-coordinated Yb^{III} cation is a distorted pentagonal bipyramid coordination polyhedron, which is coordinated by two nitrogen atoms (N1, N2) and one oxygen atom (O1B) from the sulfonic group of L^- ligand, four oxygen atoms (O4, O5A, O6C, O7B) from glu^{2-} ligands. The Yb-N and Yb-O bond lengths are in the range of 2.473(4)-2.501(4) Å and 2.219(4)-2.256(3) Å, respectively, and O-Yb-O bond angles vary from 78.02(13) to 135.64(14)°, which are similar to those reported in the Yb^{III} carboxylate compounds.[12] Differently, there is a $[Yb_2(CO_2)_4]$ subunit with Yb···Yb distance of 4.0659(5) Å because of the carboxylate group coordinating to the metallic cation. Different with compound **1**, L^- ligands

exhibit the μ_2-η^1:η^2 mode (Scheme 1b) and bridge the Yb^{III} cations to form a unique meso-helical chain running along the c axis with a pitch of 18.196Å (Figure 2b). On the other side, adjacent $[Yb_2(CO_2)_4]$ subunits are linked into an achiral 2D layer by the adjoining meso-helical chains. Finally, each binuclear $[Yb_2(CO_2)_4]$ subunit of the 2D layer is connected by glu^{2-} ligands to produce a 3D framework along the c-axis (Figure 2c). Intermolecular hydrogen bonding interactions make the 3D framework much stable (N3-H3A···O3=2.700 Å, 150.61°). Similarly, in order to make clear the analysis of the structure, we can define the binuclear $[Yb_2(CO_2)_4]$ subunits as 6-connected nodes as shown in figure 2d. The simplified structure is a 6-connected 3D network with the topological type of ***bsn***, and the point symbol is $(4^8 \cdot 5^4 \cdot 6^3)$ (Figure 2e).

Figure 2 is here

Crystal Structure of $[LnL(glu)(H_2O)]_n$ (Ln=Pr (**5**), Sm (**6**), Gd (**7**), Dy (**8**), Ho (**9**), Er (**10**), Y(**11**))**.** The seven compounds are isomorphic 2D two layer stucture in the triclinic P-1 space group. Hence, only the structure of compound **6** will be discussed in detail. The asymmetric unit consists one independent Sm^{III} cation, one L^- ligand, one glu^{2-} anion and one coordinated H_2O. As shown in Figure 3a, Sm^{III} cation is eight-coordinated by two nitrogen atoms (N1, N2) and one oxygen atom (O1B) from L^- ligand, four O atoms (O4, O5, O6C, O7D) from glu^{2-} ligands, one oxygen atom (O8) from coordinated H_2O. The Sm-N and Sm-O bond lengths are in the range of 2.601(3)-2.614(3) Å and 2.319(2)-2.500(3) Å, and O-Sm-O bond angles vary from 72.41(8) to 147.73(9)°, which are similar to those reported in the Sm^{III} carboxylate compounds.[12b,13] The adjacent Sm^{III} cations are joined by two oxygen atoms from glu^{2-} anion to show an obvious $[Sm(CO_2)]_2$ subunit, and the Sm···Sm distances is 4.395 Å. $[Sm(CO_2)]_2$ subunits are connected into 1D ringy chain by L^{-1} ligand (Figure 3b) in which L^- ligand adopt the μ_2-η^1:η^2 mode (Scheme 1b). The adjoining ringy chains are bridged glu^{2-} anions, giving rise to a 2D double layer stucture (Figures 3c and 3d). Finally, the adjoining 2D bilayers connect with each other through intermolecular hydrogen bonding interaction (O8-H8B···$O3^i$, 2.874 Å, 168.97°, symmetric code i: (-x+1, -y+2, -z+1)) and further stacked into a 3D supramolecular architecture along

the b-axis (Figure S1). The intramolecular hydrogen bond (N3-H3A···O2, 2.691 Å, 152.02°) and the intermolecular hydrogen bond (O8-H8A···O5^{ii}, 2.754 Å, 164.21°, symmetric code ii: (-x, -y+2, -z+2)) make the 3D framework much stable. If we define the $[Sm(CO_2)]_2$ subunits as 4-connected nodes (Figure 3e), the simplified structure is a 4-connected ***sql*** topology with the point symbol of $(4^4{\cdot}6^2)$ (Figure 3f).

Figure 3 is here

Crystal Structure of $[PrL(glu)(H_2O)]_n$ (**12**). X-ray crystallography reveals compound **12** is an interesting 3D network in the monoclinic $P2_1/c$ space group. The asymmetric unit contains one independent Pr^{III} cation, one L^- ligand, one glu^{2-} anion and one coordinated H_2O. The nine-coordinated Pr^{III} is a distorted tricapped trigonal prism coordination polyhedron (Figure 4a), which is coordinated by two nitrogen atoms (N1, N2) and oxygen atom (O1A) from the sulfonic group of L^- ligand, one oxygen atom (O8) from coordinated H_2O, five oxygen atoms (O4, O5, O5A, O6A, O7A) from glu^{2-} ligands. The Pr-N and Pr-O bond lengths are in the range of 2.632(2)-2.692(2) Å and 2.4062(17)-2.6458(17) Å, and O-Pr-O bond angles vary from 74.71(6) to 142.07(7)°, which are similar to those reported in the Pr^{III} carboxylate compounds.[14] It is worth noting that there is a paddle-wheel $[Pr_2O_2(CO_2)_2]$ subunit with Pr···Pr distance of 4.0749(4) Å. L^- ligands exhibit the μ_2-η^1:η^2 mode (Scheme 1b) and bridge the Pr^{III} cations to form 1D left- and right-handed helical chains of $[PrL^{-1}]_\infty$ running along the crystallographic 2_1 axis with a pitch of 13.501Å (Figure 4b). The adjoining left- and right-handed helical chains are bridged by oxygen atoms from glu^{2-} anion, giving rise to an achiral 2D layer in the ab plane. Actually, it also can be seen the binuclear $[Pr_2O_2(CO_2)_2]$ groups between each two helical chains. Finally, each binuclear $[Pr_2O_2(CO_2)_2]$ subunit of the 2D layer is connected by two glu^{2-} ligands to produce a 3D framework along the b-axis (Figure 4c). The hydrogen bonds between coordinated water molecules and L^- ligands (N3-H3A···O2, 2.819 Å, 139.26°; O8-H8A···N4^{iii}, 2.866 Å, 155.22°; O8-H8B···O3^{iv}, 2.689 Å, 164.47°; symmetric codes iii: (-x+2, -y, -z+1), iv: (-x+2, y-0.5, -z+1.5)) make the 3D framework much stable. In order to simplify the structure of **12**, we can define the binuclear $[Pr_2O_2(CO_2)_2]$ subunits as 8-connected nodes as shown in figure 4d. The

simplified structure is an 8-connected 3D network with the topological type of ***bcu***, and the point symbol of net is $(4^{24}\cdot6^{4})$ (Figure 4e).

Figure 4 is here

Analysis and comparison

All compounds were prepared under hydrothermal conditions at the same temperature. The synthetic route of **1-12** is shown as Scheme 2. Compounds **1-4** are synthesized at the pH=4.0 and the molar ratio of Ln^{III}:HL:H_2glu= 2:1:1. Compounds **1-3** show different structures with **4** because of the influence of lanthanide contraction. When only change the pH value to 6.0, isostructural compounds **5-11** can be obtained. Compound **12** are synthesized by changing the molar ratio of 2:1:1 (Ln^{III}: HL: H_2glu) to 2:1:2 at pH= 4.0. Glutaric acid plays an important role in bridging adjacent Ln^{III} cations to form a subunit. For compounds **1-3,** paddle-wheel $[Ln_2O_2(CO_2)_2]$ subunits are bridged by L^- ligands exhibiting the μ_2-η^2:η^2 mode to produce a 6-connected 3D ***pcu*** topology containing left- and right-handed helical chains. Differently, for compound **4,** $[Yb_2CO_2)_4]$ subunits are bridged by L^- ligands exhibiting the μ_2-η^1:η^2 mode to produce a 6-connected 3D ***bsn*** topology containing unique meso-helical chains. For isostructural compounds **5-11,** L^- ligands adopt the μ_2-η^1:η^2 mode to bridge $[Ln(CO_2)]_2$ subunits giving rise to a 4-connected 2D ***sql*** topology. Compound **12** is similar to **1,** in which contain $[Pr_2O_2(CO_2)_2]$ subunit and left- and right-handed helical chains. Differently, L^- ligands exhibit the μ_2-η^1:η^2 mode giving rise to an 8-connected 3D ***bcu*** topology in compound **12.**

For compounds **1-3** and **5-11**, all average Ln-O and Ln-N bond lengths desrease with the atomic numbers of Ln^{III} increasing due to the lanthanide contraction (Figure 5). The Ln···Ln distances of compounds **1-3** increase, however that of compounds **5-11** change in opposite with the increase of lanthanide atomic number. For **5-11** light lanthanide are more obvious than heavy lanthanide coordination polymers both the average Ln-O, Ln-N bond lengths and the Ln···Ln distances. Every change tendency of the curve is not a straight line, but a slightly curved upward curve as the change of the atomic numbers. This phenomenon is because the shielding effect of 4f electron increases with the electronic number.[1c,12a] with the increase of lanthanide atomic

number, the attraction of nuclear charge acting on outer electron will decrease, changes of bond distances are also becoming more slowly.

Figure 5 is here

Luminescent Properties.

Most of trivalent coordination polymers of lanthanide cations may have fluorescence when the excited state energy of rare earth cation were below the triplet energy of ligands in their coordination polymers and the energy could be transmitted efffectively.[1c,11b,12b] Figure 6 shows the emission spectra of compounds upon excitation at 370 nm at room temperature. As depicted in figure 6a, the free HL ligand displays a broad green emission band at 515 nm with CIE coordinates (0.230, 0.545). Compounds **2** and **6** display the characteristic bluish-green emissions of Sm^{III} cation from $^4G_{5/2}\rightarrow{}^6H_J$ (J = 5/2, 7/2 and 9/2) at 560, 594 and 640nm with CIE coordinates (0.207, 0.307) for **2** and (0.208, 0.297) for **6**, respectively.[13] Due to the incomplete transfer of energy from HL ligand to central Sm^{III} cation, compounds **2** and **6** appear the ligand-centered emission at 502 and 500 nm with a blue-shift of 13 and 15 nm, respectively. Compounds **3**, **7**, **8** and **11** present the ligand-centered emission at 498, 508, 496 and 500 nm with blue-shift of 17, 7, 19 and 15 nm, respectively, compared with HL ligand (Figure 6b).

The solid-state emission spectrum of compound **1** (Nd^{III}) is shown in Figure 6c. Compound **1** displays two emission bands in the range of 885-902nm and 1028-1100nm, which can be assigned to $^4F_{3/2}\rightarrow{}^4I_{9/2}$,$^4F_{3/2}\rightarrow{}^4I_{11/2}$, respectively. Besides the weak emission band at 1333 nm can assigned to $^4F_{3/2}\rightarrow{}^4I_{13/2}$.[5,15] The compound **4** displays broad emission bands of Yb^{III} in the range of 923-1025 nm (λ_{ex}= 321 nm), and the characteristic emission peak can be attributable to the transition of $^2F_{5/2}\rightarrow{}^2F_{7/2}$ at 986 nm (Figure 6d).[12b,16] Compound **9** shows the emission band of Ho^{III} at 989 nm assigning to $^5F_5\rightarrow{}^5I_7$ (Figure 6e).[17] Compounds **5**, **10** and **12** have not shown their characteristic emission peaks probably because hydrogen bonds (O···H, N···H) formed between coordinated water molecules and ligands hinder the energy transfer via the antenna effect.[1c]

Figure 6 is here

Magnetic Properties.

Magnetic susceptibility was collected in the range of 1.8−300 K and at additional field of 1000 Oe. The χ_MT vs T plots for **3**, **7**, **8**, **9** and **10** are given in Figure 7. The $\chi_M T$ values at 300 K are 8.55, 8.65, 14.53, 14.41 and 11.85 cm^3 K mol^{-1} for **3**, **7**, **8**, **9** and **10**, respectively, which are close to the expected values for two isolated Ln^{III}cations ($^8S_{7/2}$, g = 2 for Gd^{III}; $^6H_{15/2}$, g_J = 4/3 for Dy^{III}; $^5I_8$, g_J = 5/4 for Ho^{III}; $^4I_{15/2}$, g_J = 6/5 for Er^{III}).[18] With the temperature decreases, the $\chi_M T$ values of compounds **3** and **7** decrease gradually to the values of 7.26 and 7.47 cm^3 mol^{-1} K at 1.8K, respectively, which present typical paramagnetic behavior. At the region from 300 to 65 K, the $\chi_M T$ values remain roughly constant, while below 65 K, then decrease rapidly to 6.92, 3.06 and 7.69 cm^3 K mol^{-1} at 1.8 K, respectively. This is attributable to a gradual depopulation of the Stark m_J sublevels of the ground J multiplet states and/or dipolar coupling also contributing to the behavior.[19] Table S3 shows the calculated and measured values of magnetic moment for Ln^{III} cation. It is clear that measured values are in close proximity to calculated values based on J-levels in the ground stat. The influence of the environment is so small that magnetic moment of the lanthanide coordination polymers is almost the same, which is due to the shielding effect of $5s^2$ and $5p^6$ shells to the environment. [1a,1e,20]

Figure 7 is here

PXRD and Thermogravimetric analysis.

The PXRD were carried out to check the phase purity of compounds **1-12**. The measured patterns are in good agreement with simulated patterns based on the single-crystal X-ray diffraction (Figure S2).

Thermogravimetric analyses (TGA) were performed by heating up from 30 to 900 °C at 10 °C/min under a nitrogen atmosphere (Figure 8). Isomorphous compounds have similar thermal behaviors, hence only compounds **1**, **4**, **5** and **12** will

be discussed in detail. Compound **1** starts to lose two lattice water molecules at about 150 °C with the weight loss of 5.5% (calcd. 5.3%) (Figure 8a). The second weight loss of 26.9% from 380 to 610 °C can be also attributed to the complete decomposition of organic ligands (calcd. 27.4%). And then skeleton begin to collapse after the 680°C. For the compound **4** (Figure 8b), due to no coordinated or lattice water molecules, organic ligands start to decompose firstly and exhibit a loss of 22.7% (calcd. 22.5%) in the temperature range of 490-640°C. The next is the decomposition of the framework up to about 700 °C. Compounds **5** and **12** have same molecular formulas but different crystal structures (Figure 8c, d), which show same thermal behaviors. The initial weight loss of 3.1% for **12** is consistent with the calculated value (2.7%) at 200°C, corresponding to the loss of one coordinated water molecules. After the stationary phase in the temperature range of 230-450°C, a two-step weight loss of 26.3% can be attributed to the complete decomposition of organic ligands at 450°C (calcd. 25.8%), the next is the decomposition of the framework at about 700 °C. The TGA results show the four series of compounds have good thermal stability.

Figure 8 is here

Conclusion

Four series of lanthanide coordination polymers with different structures have been hydrothermally synthesized by HL ligand and glutaric acid at same temperature but different in molar ratio and pH value. With the molar ratio of 2:1:1 (Ln^{III}:HL:H_2glu), compounds **1-3** and **4** show different structures because of the influence of lanthanide contraction at pH=4.0, which are bridged by L^- ligands exhibiting the μ_2-η^2:η^2 and μ_2-η^1:η^2 modes respectively. Compounds **1-3** exhibit 6-connected 3D ***pcu*** topology, containing left- and right-handed helical chains. Differently, compound **4** is a 6-connected 3D network with ***bsn*** topology, which contains unique meso-helical chain. By changing the pH value of compounds **1-3** to 6.0, L^- ligands exhibit the μ_2-η^1:η^2 mode and are synthesized compounds **5-11** including 2D 4-connected ***sql*** topology. By changing the molar ratio of 2:1:1 (Ln^{III}:HL:H_2glu) to 2:1:2 at pH=4.0, compound **12** shows an 8-connected 3D ***bcu*** topology, containing left- and

right-handed helical chains which is different with compound **1**. It is important to control the reasonable pH value and molar ratio to synthesize coordination polymers. Besides, the influence of lanthanide contraction can't be ignored. The luminescence measurements and magnetic properties are also described in detail. The TGA results show the four series of compounds have good thermal stability.

Acknowledgements

This work was supported by the National Natural Science Foundation of China (Grant Nos. 21173164 and 21473133).

REFERENCES

(1) (a) M. Chen, E. C. Sanudo, E. Jimenez, S. M. Fang, C. S. Liu, M. Du, *Inorg. Chem.,* 2014, **53**, 6708; (b) J. Yang, C. Li, Z. Quan, C. Zhang, P. Yang, Y. Li, C. Yu, J Lin, *J. Phys. Chem. C.,* 2008, **112**, 12777; (c) S. V. Eliseeva, J. C. Bunzli, *Chem. Soc. Rev.,* 2010, **39**, 189; (d) J. C. Bunzli, C. Piguet, *Chem. Soc. Rev.,* 2005, **34**, 1048; (e) P. Zhang, L. Zhang, C. Wang, S. Xue, S. Y. Lin, J. *J.* Tang, *Am. Chem. Soc.,* 2014, **136**, 4484.

(2) (a) T. Cardinaels, J. Ramaekers, P. Nockemann, K. Driesen, K. Van Hecke, L. Van Meervelt, S. Lei, S. De Feyter, D. Guillon, B Donnio, *Chem. Mater.,* 2008, **20**, 1278; (b) J. Xia, B. Zhao, H. S. Wang, W. Shi, Y. Ma, H. B. Song, P. Cheng, D. Z. Liao, S. P. Yan, *Inorg. Chem.,* 2007, **46**, 3450.

(3) (a) Y. P. He, Y. X. Tan, J. Zhang, *Inorg. Chem.,* 2013, **52**, 12758; (b) Q. Chen, X. F. Wang, H. M. Hu, J. Wang, R. An, F. X. Dong, M. L. Yang, G. L. Xue, *Polyhedron.,* 2014, **81**, 517.

(4) (a) S. Song, X. Li, Y. H Zhang, *Dalton Trans.,* 2013, **42**, 10409; (b) Y. H. Zhang, X. Li, S. Song, *Chem. Commun.,* 2013, **49**, 10397; (c) S. Song, X. Li, Y. H. Zhang, R. Huo, D. Ma, *Dalton Trans.,* 2014, **43**, 5974.

(5) Y. Liu, L. Sun, J. Liu, Y. X. Peng, X. Ge, L. Shi, W. Huang, *Dalton Trans.,* 2015, **44**, 237.

(6) H. Tian, L. Zhao, H. Lin, J. Tang, G. Li, *Chemistry-A European Journal.,* 2013, **19**, 13235.

(7) (a) J. Wang, Q. H. Bao, H. M. Hu, B. Liu, Q. Chen, Z. H. Yang, G. L. Xue, *Z. Anorg. Allg. Chem.,* 2014, **640**, 184; (b) Q. H. Bao, Q. Chen, H. M. Hu, Y. L. Ren, B. Xu, F. X. Dong, M. L. Yang, G. L. Xue, *Inorg. Chim. Acta.,* 2013, **405**, 51.

(8) K. L. Hou, F. Y. Bai, Y. H. Xing, J. L. Wang, Z. Shi, *Inorg. Chim. Acta.,* 2011, **365**, 269.

(9) (a) K. Li, L. Y. Zhang, C. Yan, S. C. Wei, M. Pan, L. Zhang, C. Y. Su, *J. Am. Chem. Soc.,* 2014, **136**, 4456; (b) S. R. Zheng, R. L. Chen, T. Xie, Z. M. Liu, X. L. Wen, X. Y. Chen, J. Fan, W. G. Zhang, *CrystEngComm.,* 2014, **16**, 4029.

(10) (a) S. Zhang, Y. Yang, Z. Q. Xia, X. Y. Liu, Q. Yang, Q. Wei, G. Xie, S. P. Chen, S. L. Gao, *Inorg. Chem.,* 2014, **53**, 10952; (b) R. L. Chen, X. Y. Chen, S. R. Zheng, J. Fan, W. G. Zhang, *Cryst. Growth Des.,* 2013, **13**, 4428.

(11) (a) G. F. Hou, H. X. Li, W. Z. Li, P. F. Yan, X. H. Su, G. M. Li, *Cryst. Growth Des.,* 2013, **13**, 3374; (b) X. Wang, Q. G. Zhai, S. N. Li, Y. C. Jiang, M. C. Hu, *Cryst. Growth Des.,* 2014, **14**, 177; (c) Y. H. Luo, F. X. Yue, X. Y. Yu, X. Chen, H. Zhang, *CrystEngComm.,* 2013, **15**, 6340.

(12) (a) Z. He, E. Q. Gao, Z. M. Wang, C. H. Yan, M. Kurmoo, *Inorg. Chem.,* 2005, **44**, 862; (b) Z. H. Zhang, Y. Song, T. a. Okamura, Y. Hasegawa, W. Y. Sun, N. Ueyama, *Inorg. Chem.,* 2006, **45**, 2896; (c) W. J. Sun, F. Liu, W. J. Zhao, X. W. Yang, *J. Therm. Anal. Calorim.,* 2014, **1**.

(13) (a) W. Xu, Y. Zhou, D. Huang, M. Su, K. Wang, M. Xiang, M. Hong, *J. Mater. Chem. C*, 2015, **3**, 2003; (b) B. Xu, Q. Chen, H. M. Hu, R. An, X. F. Wang, G. L. Xue, *Cryst.Growth Des.*, 2015, **15**, 231

(14) (a) Y. Li, F. K. Zheng, X. Liu, W. Q. Zou, G. C. Guo, C. Z. Lu, J. S. Huang, *Inorg. Chem.,* 2006, **45**, 6308; (b) L. Sun, Y. Qiu, T. Liu, J. Z. Zhang, S. Dang, J. Feng, Z. Wang, H. Zhang, L. Shi, *ACS Appl. Mater. Interfaces.,* 2013, **5**, 9585.

(15) (a) S. Quici, M. Cavazzini, G. Marzanni, G. Accorsi, N. Armaroli, B. Ventura, F. Barigelletti, *Inorg. Chem.,* 2005, **44**, 529; (b) R. B. Fu, S. M. Hu, X. T. Wu, *Cryst.*

Growth Des., 2014, **14**, 6197; (c) L. Y. Zhang, T. Y. Song, J. N. Xu, J. Y. Sun, S. L. Zeng, Y. C. Wu, Y. Fan, L. Wang, *CrystEngcomm.,* 2014, **16**, 2440.

(16) (a) F. Artizzu, F. Quochi, L. Marchio, C. Figus, D. Loche, M. Atzori, V. Sarritzu, A. M. Kaczmarek, R. Van Deun, M. Saba, A. Serpe, A. Mura, M. L. Mercuri, G. Bongiovanni, P. Deplano,*Chem. Mat.,* 2015, **27**, 4082; (b) G. Jalani, R. Naccache, D. H. Rosenzweig, S. Lerouge, L. Haglund, F. Vetrone, M. Cerruti, *Nanoscale.,* 2015, **7**, 11255; (c) V. V. Utochnikova, A. D. Kovalenko, A. S. Burlov, L. Marciniak, I. V. Ananyev, A. S. Kalyakina, N. A. Kurchavov, N. P. Kuzmina, *Dalton Trans.,* 2015, **44**, 12660.

(17) (a) Z. Ahmed, K. *J.* Iftikhar, *Phys. Chem. A.,* 2013, **117**, 11183; (b) Y. X. Chi, T. S. Liu, J. Jin, G. N. Zhang, S. Y. Niu, *J. Phys. Chem. Solids.,* 2013, **74**, 1745; (c) L. F. Marques, C. C. Correa, S. J. L. Ribeiro, M. V. Santos, J. D. L. Dutra, R. O. Freire, F. C. Machado, *J. Solid State Chem.,* 2015, **227**, 68.

(18) B. M. Ji, D. S. Deng, X. He, B. Liu, S. B. Miao, N. Ma, W. Z. Wang, L. G. Ji, P. Liu, X. F. Li, *Inorg. Chem*., 2012, **51**, 2170; (b) X. Feng, J. S. Zhao, B. Liu, L. Y. Wang, S. K. Ng, G. Zhang, J. G. Wang, X. G. Shi, Y. Y. Liu, *Cryst. Growth Des.,* 2010, **10**, 1399.

(19) (a) S. M. Abtab, M. C. Majee, M. Maity, J. Titis, R. Boca, M. Chaudhury, *Inorg. Chem.,* 2014, **53**, 1295; (b) Y. L. Ren, F. Wang, H. M. Hu, Z. Chang, M. L. Yang, G. L. Xue, *Inorg. Chim. Acta.,* 2015, **434**, 104; (b) X. Feng, Y. Q. Feng, J. J. Chen, S. W. Ng, L. Y. Wang, J. Z. Guo, *Dalton Trans.,* 2015, **44**, 804.

(20) (a) M. F. Wu, M. S. Wang, S. P. Guo, F. K. Zheng, H. F. Chen, X. M. Jiang, G. N. Liu, G. C. Guo, J. S. Huang, *Cryst. Growth Des.,* 2011, **11**, 372; (b) S. Chorazy, M. Arczynski, K. Nakabayashi, B. Sieklucka, S. Ohkoshi, *Inorg. Chem.,* 2015, **54**, 4724;

Figure Captions:

Table 1. Crystal data and structural refinement parameters for compounds **2**, **4**, **6** and **12**.

Scheme 1. The coordination modes of L^-.

Scheme 2. Reaction routes of compounds **1-12**.

Figure 1. (a) Coordination environment of Sm^{III} cation in **2**. The hydrogen atoms are omitted for clarity. (b) The achiral 2D layer containing the adjoining left- and right-handed helical chains. (c) The 3D framework along the b-axis. (d) The binuclear $[Sm_2O_2(CO_2)_2]$ subunits were simplified as 6-connected nodes. (e) The $(4^{12}\cdot6^3)$ topological type of ***pcu***. Symmetry codes: A = (1-x, 1-y, -z); B = (1.5-x, -0.5+y, 0.5-z); C = (x-1, y, z); D = (2-x, 1-y, -z).

Figure 2. (a) Coordination environment of Yb^{III} cation in **4**. The hydrogen atoms are omitted for clarity. (b) The 2D layer containing meso-helical chains along the ab plane. (c) The 3D framework constructed by connecting binuclear $[Yb_2(CO_2)_4]$ subunits by oxygen atoms from glu^{2-} anion along the c-axis. (d) The binuclear $[Yb_2(CO_2)_4]$ subunit were simplified as 6-connected nodes. (e) The $(4^8\cdot5^4\cdot6^3)$ topological type of ***bsn***. Symmetry codes: A = (1-x, 2-y, z); B = (1-x, 2-y, z-1); C = (x, y, z-1); D = (1.25-x, 0.25+y, 0.25+z).

Figure 3. (a) Coordination environment of Sm^{III} cation in **6**. The hydrogen atoms are omitted for clarity. (b)The $[Sm(CO_2)]_2$ subunits are connected into 1D ringy chain by L^{-1} ligand. (c,d) The 2D double layer stucture in the ac and bc planes. (e) The binuclear $[Sm(CO_2)]_2$ subunit were simplified as 4-connected nodes. (f) The $(4^4\cdot6^2)$ topological type of ***sql***. Symmetry codes: A = (x, y-1, z); B = (-x, 2-y, 1-z); C = (x, 1+y, z); D = (-x, 1-y, 2-z).

Figure 4. (a) Coordination environment of Pr^{III} cation in **12**. The hydrogen atoms are omitted for clarity. (b) The achiral 2D layer containing the adjoining left- and right-handed helical chains along the ab plane. (c) The 3D framework along the b-axis. (d) The binuclear $[Pr_2O_2(CO_2)_2]$ subunits were simplified as 8-connected nodes. (e)

The ($4^{24}\cdot6^4$) topological type of ***bcu***. Symmetry codes: A = (-1+x, -y, 1-z); B = (2-x, y-0.5, 1.5-z); C = (1-x, y-0.5, 0.5-z); D = (x, 0.5-y, 0.5+z).

Figure 5.The average Ln-O, Ln-N bond lengths and the Ln···Ln distances of complexes **1**-**3** and **5**-**11**.

Figure 6. Solid-state emission spectra of compounds **1**(Nd^{III}), **2** (Sm^{III}), **3**(Gd^{III}), **4**(Yb^{III}), **6**(Sm^{III}), **7**(Gd^{III}), **8**(Dy^{III}), **9**(Ho^{III}), **11**(Y^{III}) and HL ligand, respectively (λ_{ex}=370 nm).

Figure 7. Temperature dependence of $\chi_M T$ for compounds **3**, **7**, **8**, **9** and **10** respectively.

Figure 8. Thermogravimetric analyses for compounds **1**-**12.**

Table 1. Crystal data and structural refinement parameters for **2**, **4**, **6** and **12**.

compound	**2**	**4**	**6**	**12**
empirical formula	$SmC_{24}H_{21}N_4O_9S$	$YbC_{24}H_{17}N_4O_7S$	$SmC_{24}H_{19}N_4O_8S$	$PrC_{24}H_{19}N_4O_8S$
formula weight	690.82	678.51	673.84	664.40
crystal system	Orthorhombic	Orthorhombic	Triclinic	Monoclinic
space group	$P2_1/n$	F d d 2	P-1	$P2_1/c$
a (Å)	8.2415(8)	30.013(3)	9.0064(9)	13.6008(12)
b (Å)	14.9167(15)	35.346(6)	9.0831(10)	13.5013(12)
c (Å)	20.773(2)	8.6690(9)	14.4399(14)	13.1330(12)
α (°)	90	90	95.147(2)	90
β (°)	98.860(2)	90	91.280(2)	96.2310(10)
γ (°)	90	90	99.0760(10)	90
V (Å^3)	2523.2(4)	9196(2)	1161.0(2)	2397.3(4)
Z	4	16	2	4
ρ_{calcd} (mg·m^{-3})	1.808	1.960	1.928	1.841
μ (mm^{-1})	2.471	4.215	2.680	2.179
F(000)	1352	5296	666	1320
collected / unique	12309 / 4449	11312 / 3863	5763 / 4025	11588 / 4216
$R_{(int)}$	0.0297	0.0362	0.0171	0.0285
parameters	352	334	349	349
S on F^2	1.023	0.949	1.059	1.048
R_1, wR_2 [I>2σ(I)]	0.0267, 0.0604	0.0223, 0.0420	0.0241, 0.0552	0.0216, 0.0456
R_1, wR_2 (all data)	0.0337, 0.0636	0.0254, 0.0432	0.0265, 0.0570	0.0274, 0.0475
$\Delta\rho_{max\ and\ min}$(e.Å^{-3})	0.610 and -0.670	0.304 and -0.473	0.501 and -0.657	0.742 and -0.452

Scheme 1. The coordination modes of L^-.

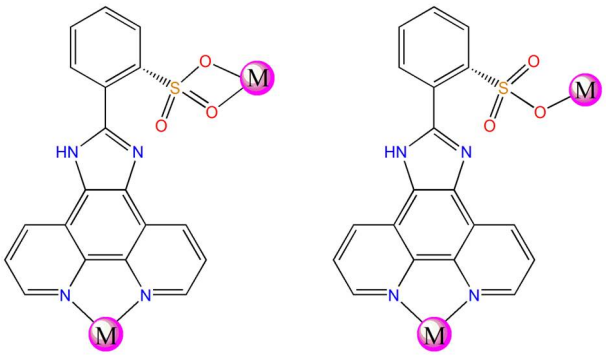

Scheme 2. Reaction routes of compounds **1-12**.

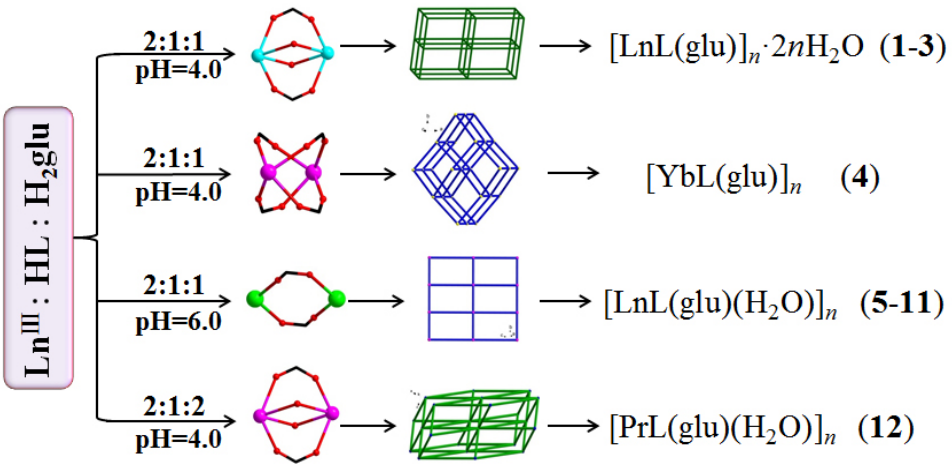

Figure 1. (a) Coordination environment of Sm^{III} cation in **2**. The hydrogen atoms are omitted for clarity. (b) The achiral 2D layer containing the adjoining left- and right-handed helical chains. (c) The 3D framework along the b-axis. (d) The binuclear $[Sm_2O_2(CO_2)_2]$ subunits were simplified as 6-connected nodes. (e) The $(4^{12}\cdot6^3)$ topological type of ***pcu***. Symmetry codes: A = (1-x, 1-y, -z); B = (1.5-x, -0.5+y, 0.5-z); C = (x-1, y, z); D = (2-x, 1-y, -z).

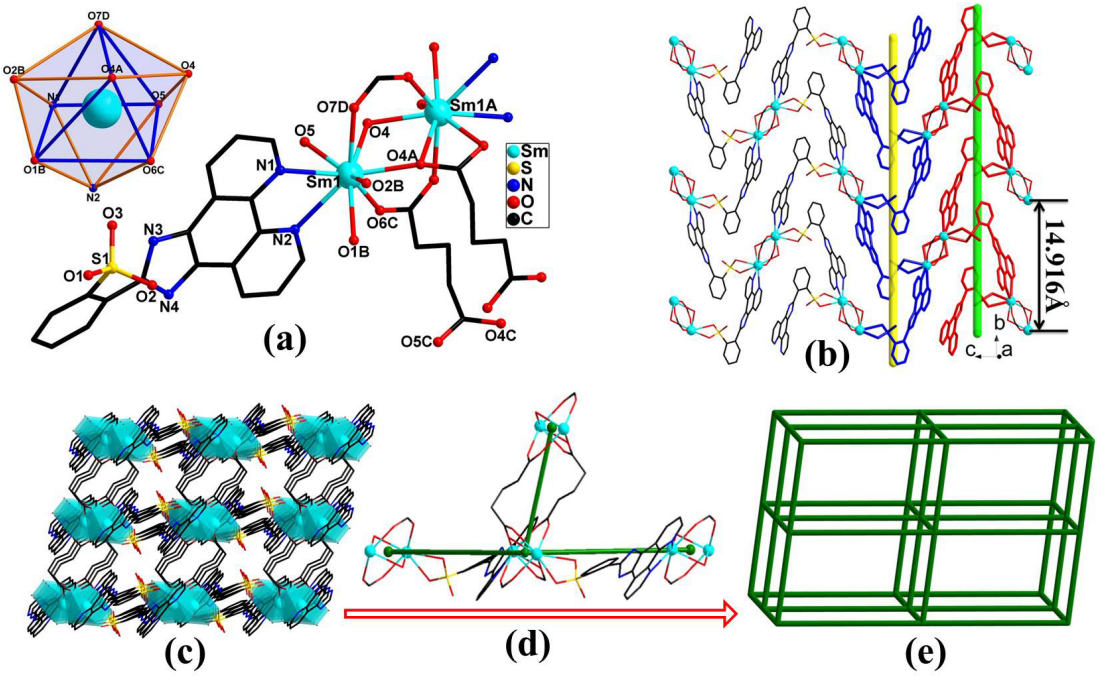

Figure 2. (a) Coordination environment of Yb^{III} cation in **4**. The hydrogen atoms are omitted for clarity. (b) The 2D layer containing meso-helical chains along the ab plane. (c) The 3D framework constructed by connecting binuclear $[Yb_2(CO_2)_4]$ subunits by oxygen atoms from glu^{2-} anion along the c-axis. (d) The binuclear $[Yb_2(CO_2)_4]$ subunit were simplified as 6-connected nodes. (e) The $(4^8 \cdot 5^4 \cdot 6^3)$ topological type of ***bsn***. Symmetry codes: A = (1-x, 2-y, z); B = (1-x, 2-y, z-1); C = (x, y, z-1); D = (1.25-x, 0.25+y, 0.25+z).

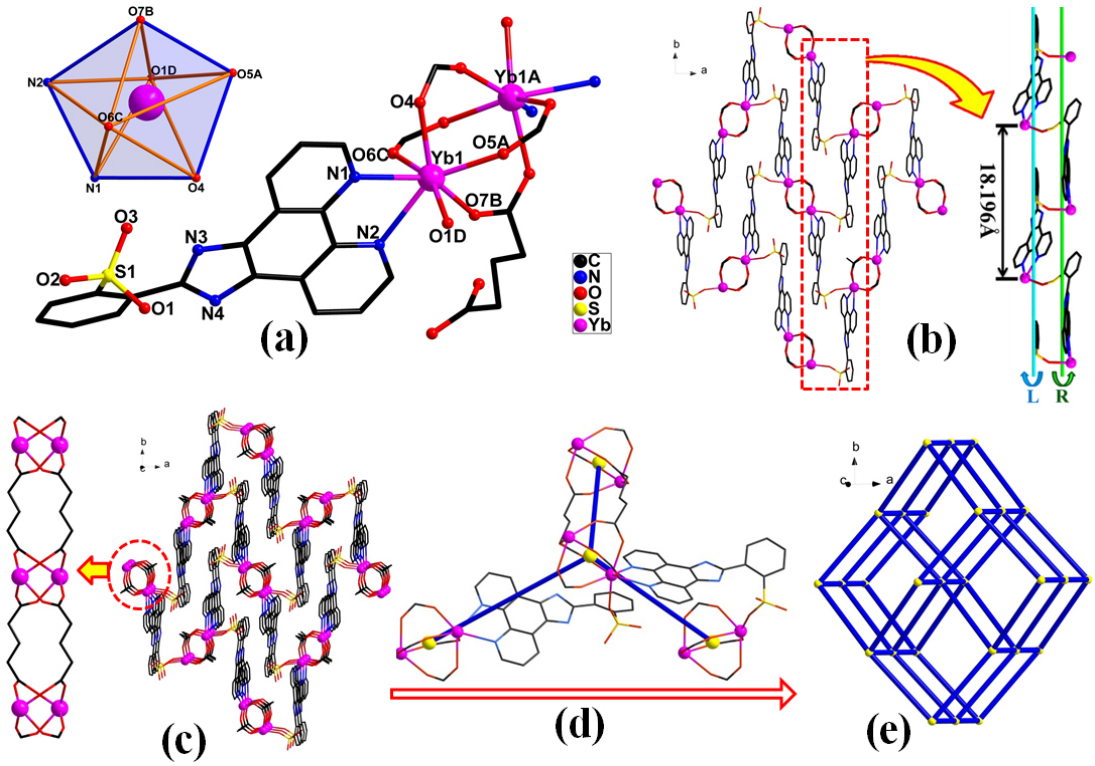

Figure 3. (a) Coordination environment of Sm^{III} cation in **6**. The hydrogen atoms are omitted for clarity. (b)The $[Sm(CO_2)]_2$ subunits are connected into 1D ringy chain by L^{-1} ligand. (c,d) The 2D double layer stucture in the ac and bc planes. (e) The binuclear $[Sm(CO_2)]_2$ subunit were simplified as 4-connected nodes. (f) The $(4^4 \cdot 6^2)$ topological type of ***sql***. Symmetry codes: A = (x, y-1, z); B = (-x, 2-y, 1-z); C = (x, 1+y, z); D = (-x, 1-y, 2-z).

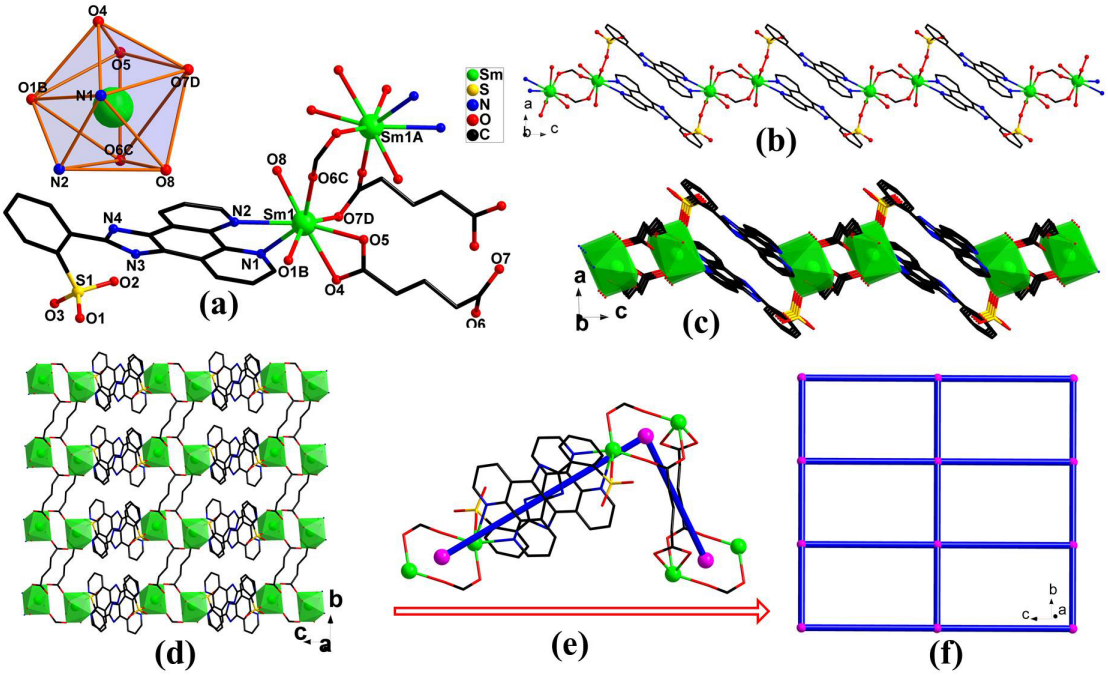

Figure 4. (a) Coordination environment of Pr^{III} cation in **12**. The hydrogen atoms are omitted for clarity. (b) The achiral 2D layer containing the adjoining left- and right-handed helical chains along the ab plane. (c) The 3D framework along the b-axis. (d) The binuclear $[Pr_2O_2(CO_2)_2]$ subunits were simplified as 8-connected nodes. (e) The $(4^{24}\cdot6^4)$ topological type of ***bcu***. Symmetry codes: A = (-1+x, -y, 1-z); B = (2-x, y-0.5, 1.5-z); C = (1-x, y-0.5, 0.5-z); D = (x, 0.5-y, 0.5+z).

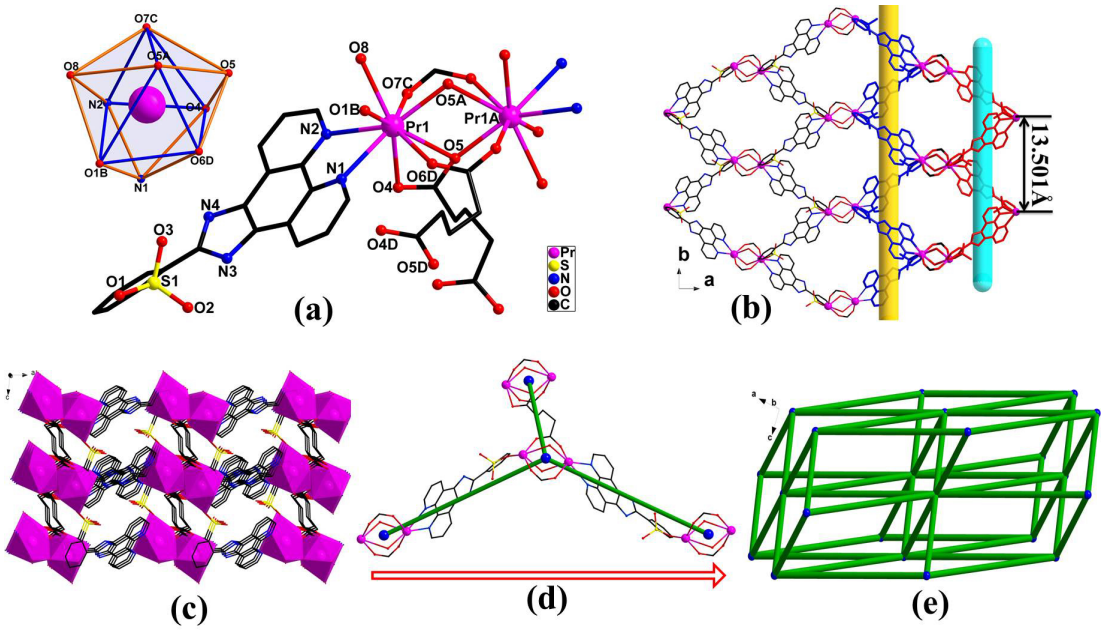

Figure 5.The average Ln-O, Ln-N bond lengths and the Ln···Ln distances of complexes **1-3** and **5-11**.

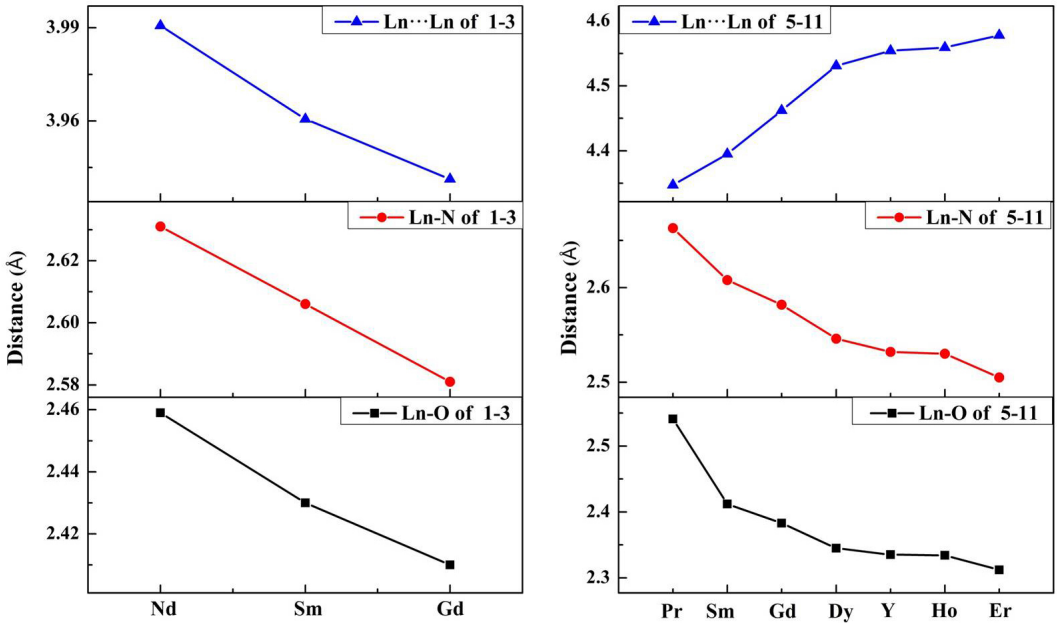

Figure 6. Solid-state emission spectra of compounds **1**(Nd^{III}), **2** (Sm^{III}), **3**(Gd^{III}), **4**(Yb^{III}), **6**(Sm^{III}), **7**(Gd^{III}), **8**(Dy^{III}), **9**(Ho^{III}), **11**(Y^{III}) and HL ligand, respectively (λ_{ex}=370 nm).

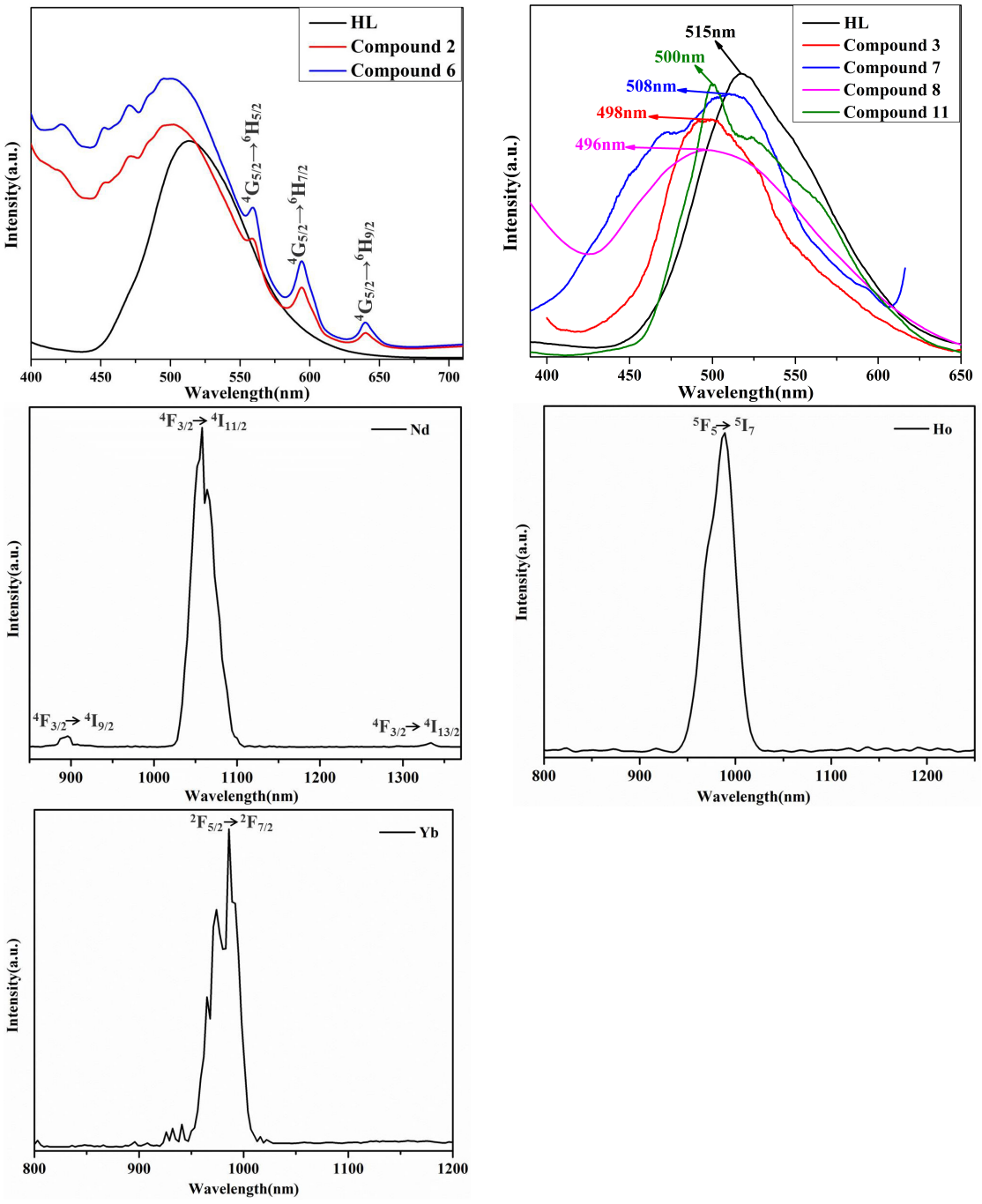

Figure 7. Temperature dependence of $\chi_M T$ for compounds **3**, **7**, **8**, **9** and **10** respectively.

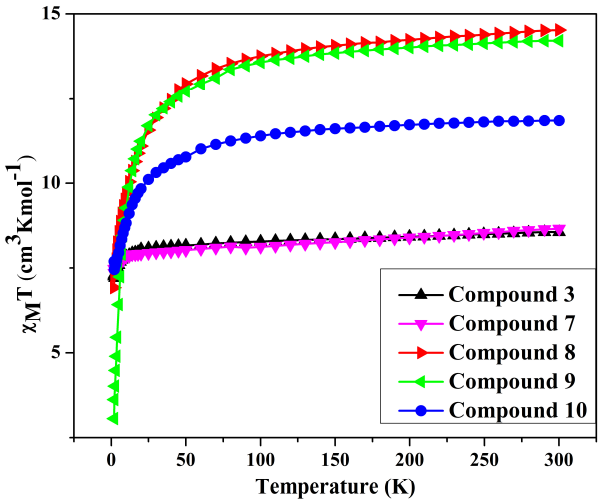

Figure 8. Thermogravimetric analyses for compounds **1-12.**